curved crystals, and a high brilliance in those experiments that do.

Many surveys of existing and planned synchrotron-radiation sources have been published since the compilation of Table 4.2.1.6. Figure 4.2.1.11, taken from a recent review (Suller, 1992), is a graphical illustration of the growth and the distribution of these sources. An earlier census is due to Huke & Kobayakawa (1989). Many detailed descriptions of beam lines for particular purposes, such as protein crystallography (*e.g* Fourme, 1992) or at individual storage rings (*e.g*. Kusev, Raiko & Skuratowski, 1992) have appeared: these are too numerous to list here and can be located by reference to *Synchrotron Radiation News*.

4.2.1.6. *Plasma X-ray sources*

Plasma sources of hard X-rays are being investigated in many laboratories. Most of the material in this section is derived from publications from the Laboratory for Laser Energetics, University of Rochester, USA. Plasma sources of very soft X-rays have been reviewed by Byer, Kuhn, Reed & Trail (1983).

The peak wavelength of emission from a black-body radiator falls into the ultraviolet at about 10^5 K and into the X-ray region between 10^6 and 10^7 K. At these temperatures, matter is in the form of a plasma that consists of highly ionized atoms and of electrons with energies of several keV. The only successful methods of heating plasmas to temperatures in excess of 10^6 K is by means of high-energy laser beams with intensities of 10^{12} W mm^{-2} or more. The duration of the laser pulse must be less than 1 ns so that the plasma cannot flow away from the pulse. When the plasmas are created from elements with $15 < Z < 25$, they consist mainly of ions stripped to the *K* shell, that is of hydrogen- and helium-like ions. The X-ray spectrum (Fig. 4.2.1.12) then contains a main group of lines with a bandwidth for the group of about 1%; the band is situated slightly below the *K*-absorption edge of the target material. The intensity of the band drops with increasing atomic number. For diffraction studies, Forsyth & Frankel (1980, 1984) and Frankel & Forsyth (1979, 1985) used a multi-stage Nd^{3+}:glass laser (Seka, Soures, Lewis, Bunkenburg, Brown, Jacobs, Mourou & Zimmermann, 1980), which was able to deliver up to 220 J per pulse of width 700 ps. They obtained 6×10^{14} photons pulse^{-1} for a Cl^{15+} plasma with a mean wavelength of about 4.45 Å and about 3×10^{13} photons pulse^{-1} for a Fe^{24+} plasma at about 1.87 Å (Yaakobi, Bourke, Conturie, Delettrez, Forsyth, Frankel, Goldman, McCrory, Seka, Soures, Burek & Deslattes, 1981). More recently, the laser was fitted

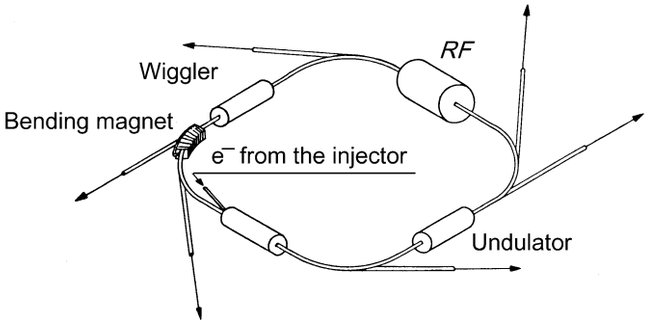

Fig. 4.2.1.7. Main components of a dedicated electron storage-ring synchrotron-radiation source. For clarity, only one bending magnet is shown. From Buras & Tazzari (1984); courtesy of ESRP.

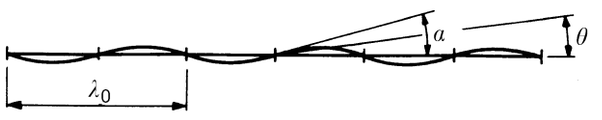

Fig. 4.2.1.8. Electron trajectory within a multipole wiggler or undulator. λ_0 is the spatial period, α the maximum deflection angle, and θ the observation angle. From Buras & Tazzari (1984); courtesy of ESRP.

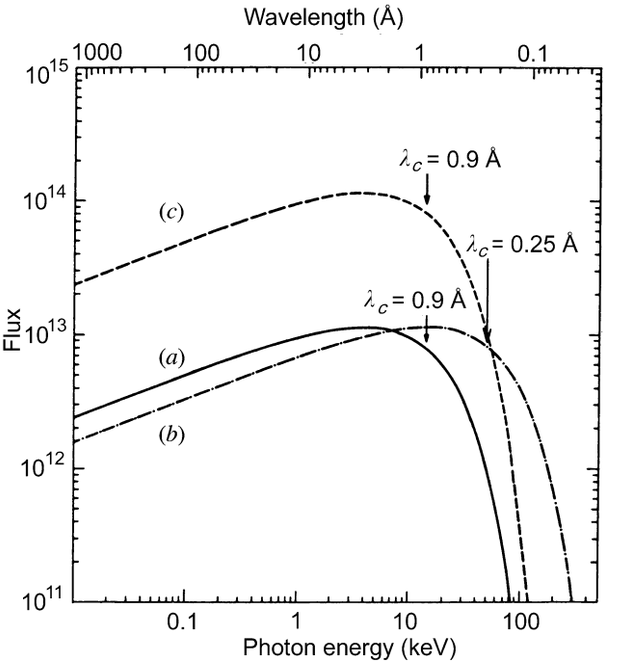

Fig. 4.2.1.9. Spectral distribution and critical wavelengths for (*a*) a dipole magnet, (*b*) a wavelength shifter, and (*c*) a multipole wiggler for the proposed ESRF. From Buras & Tazzari (1984); courtesy of ESRP.

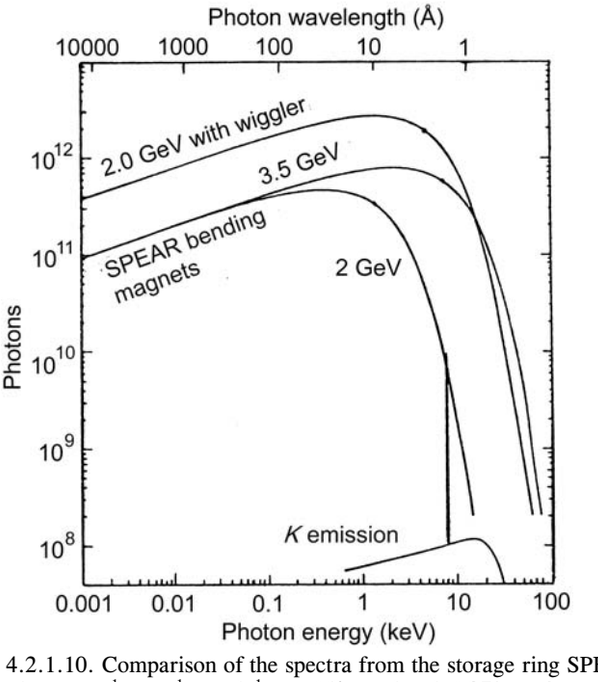

Fig. 4.2.1.10. Comparison of the spectra from the storage ring SPEAR in photons s^{-1} mA^{-1} mrad^{-1} per 1% passband (1978 performance) and a rotating-anode X-ray generator. From Nagel (1980); courtesy of K. O. Hodgson.

Table 4.2.1.6. *Comparison of storage-ring synchrotron-radiation sources; the parameters were correct in 1985 and, for some sources, may be substantially different from those at earlier or later periods; after Buras & Tazzari (1984), courtesy of ESRP*

Storage ring	Source type	No. of poles	I (mA)	E (GeV)	R (m)	σ_x (mm)*	σ_z (mm)*	σ'_z (mrad)*	λ_c (Å)	$E_{c(\mathrm{keV})}$	Flux $\left[\frac{\text{photons s}^{-1}}{\text{mrad} \times 0.1\%\ \text{BW}}\right]$ at λ^c	Flux at 1.54 Å
(1) ESRF	BM	–	100	5.0	20.0	0.092	0.100	0.008	0.9	14	8×10^{12}	1×10^{13}
(2) ESRF	W	30	100	5.0	11.56	0.062	0.040	0.016	0.5	24	2.4×10^{14}	3×10^{14}
(3) ADONE (Frascati)	BM	–	100	1.5	5.0	0.8	0.4	0.04	8.0	1.5	2.4×10^{12}	5×10^{10}
(4) ADONE (Frascati)	W	6	100	1.5	2.6	1.4	0.24	0.08	4.3	3	1.4×10^{13}	3.4×10^{12}
(5) SRS (Daresbury)	BM	–	300	2.0	5.56	2.7	0.23	0.05	4.0	3	1×10^{13}	3×10^{12}
(6) SRS (Daresbury)	W	1	300	2.0	1.33	5.3	0.17	0.05	0.9	13	1×10^{13}	1.2×10^{13}
(7) DCI (Orsay)	BM	–	250	1.8	3.82	2.72	1.06	0.06	3.6	3.4	7×10^{12}	2.4×10^{12}
(8) DORIS (Hamburg)	BM	–	100	3.7	12.22	1.0	0.3	0.05	1.3	9.2	6×10^{12}	6.4×10^{12}
(9) DORIS (Hamburg)	BM	–	40	5.0	12.22	1.3	0.65	0.065	0.55	23	3×10^{12}	4.4×10^{13}
(10) DORIS (Hamburg)	W	32	100	3.7	20.57	1.5	0.4	0.033	2.3	5.5	1.9×10^{14}	1.3×10^{14}
(11) CESR (Cornell)	BM	–	40	5.5	32.0	1.44	1.0	0.065	1.0	11.5	3.5×10^{12}	4×10^{12}
(12) CESR (Cornell)	W	6	40	5.5	13.2	1.9	1.2	0.05	0.4	28	2×10^{13}	3×10^{13}
(13) NSLS X-ray (Brookhaven)	BM	–	300	2.5	6.83	0.25	0.1	0.01	2.4	5	1×10^{13}	8×10^{12}
(14) SPEAR	BM	–	100	3.0	12.7	2.0	0.28	0.05	2.7	5	5×10^{12}	3×10^{12}
(15) SPEAR	W	8	100	3.0	5.57	3.2	0.15	0.03	1.0	10	3.8×10^{13}	4.5×10^{13}
(16) SPEAR	W	54	100	3.0	8.36	3.2	0.15	0.03	1.7	7	2.6×10^{14}	2.4×10^{14}
(17) Photon Factory (Tsukuba)	BM	–	150	2.5	8.66	2.2	0.6	0.14	3.0	4	6×10^{12}	3×10^{12}
(18) Photon Factory (Tsukuba)	W	3	150	2.5	1.85	1.9	0.7	0.18	0.7	19	1.8×10^{13}	2.5×10^{13}
(19) VEPP-3	BM	–	100	2.2	6.15	6.15	0.08	0.02	3.0	4	3.5×10^{12}	1.5×10^{12}

* One standard deviation of Gaussian distribution.

with a frequency conversion system that shifts the peak power of the laser light from the infrared (1.054 μm) to the ultraviolet (0.351 μm) (Seka, Soures, Lund & Craxton, 1981). This led to a more efficient X-ray production, which permitted a more than twofold increase in X-ray flux, even though the maximum pulse energies had to be reduced to ~ 50 J to prevent damage to the optical components (Yaakobi, Boehli, Bourke, Conturie, Craxton, Delettrez, Forsyth, Frankel, Goldman, McCrory, Richardson, Seka, Shvarts & Soures, 1981). Forsyth & Frankel (1984) used the plasma X-ray source for diffraction studies with 4.45 Å X-rays with a focusing collimation system that delivered up to 10^{10} photons pulse^{-1} to the specimen over an area approximately 150 μm in diameter. More recently, by special target design (Forsyth, 1986, unpublished), fluxes have been increased by factors of 2 to 3 without altering the laser output. Other plasma sources have been described by Collins, Davanloo & Bowen (1986) and by Rudakov, Baigarin, Kalimin, Korolev & Kumachov (1991).

The cost of plasma sources is about an order of magnitude greater than that of rotating-anode generators (Nagel, 1980). Their use is at present confined to flash-diffraction experiments, since the duty cycle is a maximum of one flash every 30 min. Attempts are being made to increase the laser repetition rate; a substantial improvement could lead to a source that would rival storage-ring sources.

4.2.1.7. *Other sources of X-rays*

Parametric X-ray generation can be described as the diffraction of virtual photons associated with the field of a relativistic charged particle passing through a crystal. These diffracted photons appear as real photons with an energy that satisfies Bragg's law for the reflecting crystal planes, so that the energy can be tuned between 5 and 45 keV by rotating the mosaic graphite crystal. Linear accelerators with an energy between 100 and 500 MeV produce the incident relativistic electron beam (Maruyama, Di Nova, Snyder, Piestrup, Li, Fiorito & Rule, 1993; Fiorito, Rule, Piestrup, Li, Ho & Maruyama, 1993).

Transition-radiation X-rays with peak energies between 10 and 30 keV are produced when electrons from 100 to 400 MeV strike a stack of thin foils (Piestrup, Moran, Boyers, Pincus, Kephart, Gearhart & Maruyama, 1991). Quasi-monochromatic X-rays result from a selection of target foils with appropriate *K*-, *L*- or *M*-edge frequencies (Piestrup, Boyers, Pincus, Harris, Maruyama, Bergstrom, Caplan, Silzer & Skopic, 1991).

references